Acta Radiologica Open
5(6) 1–7

DOI: 10.1177/2058460116645375
arr.sagepub.com
SAGE

# Usefulness of T2*-weighted MRI in the detection of adnexal torsion

**Nobuyuki Kawai[1], Hiroki Kato[1], Masayuki Kanematsu[1], Shimpei Kawaguchi[2], Toshihisa Kojima[2], Tatsuro Furui[3], Ken-ichirou Morishige[3] and Masayuki Matsuo[1]**

## Abstract

**Background:** The usefulness of T2*-weighted (T2*W) imaging for the detection of adnexal torsion has yet to be determined.

**Purpose:** To assess the usefulness of T2*W imaging for detecting and differentiating adnexal torsion.

**Material and Methods:** Eight patients with eight ovaries with torsion and 44 patients with 72 ovaries without torsion were included in this study. All patients underwent 1.5-T magnetic resonance imaging (MRI) including T2*W images. The frequency and distribution of hypointensity on T2*W images were compared between ovaries with torsion and ovaries without torsion.

**Results:** Hypointensity on T2*W images was significantly more frequent in ovaries with torsion than in ovaries without torsion (75% vs. 36%; $P < 0.05$). Among patients with hypointensity on T2*W images, the frequency of diffuse hypointensity was significantly higher in ovaries with torsion than in ovaries without torsion (83% vs. 0%; $P < 0.01$); whereas the frequency of focal hypointensity was significantly lower in ovaries with torsion than in ovaries without torsion (17% vs. 100%; $P < 0.01$).

**Conclusion:** The presence and distribution of hypointensity on T2*W images may play a supplementary role in the detection of adnexal torsion.

**Keywords**
Adnexal torsion, magnetic resonance imaging (MRI), T2*-weighted images

Date received: 22 March 2016; accepted: 28 March 2016

## Introduction

Adnexal torsion is uncommon and is estimated to occur in only 2.7% of gynecologic emergencies in the United States (1). A delay in the diagnosis of torsion results in loss of ovarian function, underscoring the necessity for urgent surgical intervention to prevent ovarian infarction and necrosis. However, the clinical and laboratory manifestations of adnexal torsion are often nonspecific, commonly leading to delay in the diagnosis and surgical management. Although ultrasonography is the primary imaging modality for evaluation of adnexal torsion (2), computed tomography (CT) or magnetic resonance imaging (MRI) may also serve as tools if the diagnosis remains unclear (3). MRI is particularly helpful in young or pregnant patients with equivocal sonographic findings, as it provides excellent soft tissue contrast without radiation exposure (4). The characteristic MRI findings of adnexal torsion have been described as follows: fallopian tube thickening; whirlpool sign (a twisted ovarian pedicle or twisted fallopian tube); enlargement of the ovarian stroma; peripheral ovarian follicles; symmetrical or asymmetrical wall thickening of the twisted ovarian cystic mass;

[1]Department of Radiology, Gifu University School of Medicine, Gifu, Japan
[2]Department of Radiology, Gifu Municipal Hospital, Gifu, Japan
[3]Department of Obstetrics and Gynecology, Gifu University School of Medicine, Gifu, Japan

**Corresponding author:**
Hiroki Kato, Department of Radiology, Gifu University School of Medicine 1-1 Yanagido, Gifu 501-1194, Japan.
Email: hkato@gifu-u.ac.jp

uterine deviation towards the side of torsion; and free fluid (3–9).

Susceptibility-weighted imaging provides superior sensitivity in detecting hemorrhage compared with conventional spin-echo sequences (10). T2*-weighted (T2*W) gradient-echo imaging is one of the susceptibility-weighted imaging sequences, that are widely used to evaluate hemorrhagic foci or mineralization, particularly in the brain (11). Due to its high sensitivity to the magnetic susceptibility effect, even micro hemorrhages can be detected as small signal intensity loss on T2*W images (12). As a hematoma ages, hemoglobin passes through several forms, such as oxyhemoglobin, deoxyhemoglobin, and methemoglobin, prior to red cell lysis and breakdown into ferritin and hemosiderin (13,14). T2*W imaging helps detect early signal intensity changes that are attributed to deoxymethemoglobin, which is produced immediately after extravasation (15).

Adnexal torsion is usually associated with reduced venous return from the ovary, resulting in stromal edema and internal hemorrhage. Although susceptibility-weighted imaging of subacute ovarian torsion has been reported in a case report (16), we were unable to find any previous reports that assessed the imaging findings and diagnostic value of T2*W images for adnexal torsion. Therefore, this study aimed to assess the usefulness of T2*W imaging in the detection of adnexal torsion.

## Material and Methods

### Patients

This study was approved by our institutional review board and complied with the guidelines of the Healthcare Insurance Portability and Accountability Act. Written informed consent was waived because this study was retrospective. The registries of two institutions from January 2013 to December 2014 were searched for consecutive pre-menopausal women who underwent gynecological 1.5-T MRI, including T2*W imaging. From a total of 60 records identified, eight were excluded from this study because of non-visualization of the bilateral ovarian stroma on MR images, probably due to oophorectomy, atrophy, or compression of ovarian mass. Thus, a total of 52 pre-menopausal women (mean age, 37 years; age range, 10–49 years) were included in this study. Among them, the diagnosis of adnexal torsion was proven in eight patients by laparoscopic surgery. The patients were grouped according to the presence or absence of adnexal torsion. In 44 patients without adnexal torsion, 16 ovaries were excluded because ovarian stroma was not identified. The details of 16 excluded ovaries could be summarized as follows: five endometriomas, seven benign cystic lesions, two hemorrhagic follicles, one malignant tumor, and one ovarian atrophy. There were eight patients (mean age, 29 years; age range, 10–43 years) with eight ovaries with torsion and 44 patients (mean age, 39 years; age range, 10–49 years) with 72 ovaries without torsion.

All eight patients with adnexal torsion presented with lower abdominal pain. The interval between onset of abdominal pain and MR examination was in the range of 5.6–113.6 h (mean, 37.0 h) and the interval between MR examination and surgery was in the range of 0.8–8.9 h (mean, 3.7 h). Adnexal torsion occurred on the right side in five patients (63%) and on the left in three patients (37%). Ovarian rotation was in the range of 180–720 degrees (mean, 383 degrees). Severe hemorrhagic infarction was found on pathologic examination of the twisted ovary in three of eight (38%) patients. In the remaining five patients, the diseased ovary was salvaged by repair of torsion. Four (50%) ovaries with torsion had no mass lesion, whereas the remaining four (50%) were accompanied by a benign ovarian lesion, namely, mature cystic teratoma (n = 1), serous cystadenoma (n = 1), mucinous cystadenoma (n = 1), and hemorrhagic corpus luteum cyst (n = 1).

### MRI

MRI was performed using a 1.5-T MRI system (Intera Achieva 1.5 T Pulsar, Philips Medical Systems, Best, The Netherlands) with a phased-array body coil (16-channel torso array coil) to allow whole pelvic coverage. All images were obtained in the transaxial plane using parallel imaging at a section thickness of 5 mm with a 2-mm intersection gap and field of view of 28 cm × 90%. T1-weighted (T1W) turbo spin-echo (repetition time [TR]/echo time [TE], 607 /10 ms; flip angle, 90°; matrix size, 352 × 70%), fat-suppressed T1W turbo spin-echo (TR/TE, 681 /10 ms; flip angle, 90°; matrix size, 352 × 70%), T2-weighted (T2W) turbo spin-echo (TR/TE, 4415/100 ms; flip angle, 90°; matrix size, 400 × 70%), T2*W gradient-echo (TR/TE, 476/19 ms; flip angle, 25°; matrix size, 304 × 80%) images were obtained for all patients.

### Image analysis

Two independent experienced radiologists with 16 years and 4 years in post-training experience in gynecological MRI, who were unaware of the patients' clinical information, retrospectively reviewed the MR images. Any disagreement between the reviewers was resolved through consensus.

The radiologists assessed for hypointensity within the ovarian stroma on T2*W images. The distribution

of hypointensity was recorded according to the following classification: I = localized (solitary or few); IA = ring-shaped or arc-shaped hypointensity at the periphery of the follicles (Fig. 1); IB = punctate hypointensity at the periphery of the follicles or within the ovarian stroma (Fig. 2); IC = patchy hypointensity within the ovarian stroma (Fig. 3); II = diffuse (multiple), diffuse hypointensity at the periphery of the follicles and within ovarian stroma (Figs 4 and 5).

The reviewers also measured the maximum diameter of ovarian stroma, the number of follicles, and maximum diameter of follicles. The ovarian stroma could be confirmed in all eight torsed ovaries. In all four torsed ovaries with ovarian mass, we could observe crescent-shaped stromal edema at the periphery of ovarian mass. In eight patients with adnexal torsion, the presence of fallopian tube thickening, uterine deviation to the side of torsion, and hemoperitoneum were also assessed.

### *Statistical analysis*

All statistical analyses were performed using SPSS for Windows (version 18.0, SPSS Inc., Chicago, IL, USA). Chi-square test or Fisher's exact test was performed to compare the frequencies and distributions of hypointensity on T2*W images between ovaries with torsion and ovaries without torsion. Unpaired *t*-test was used

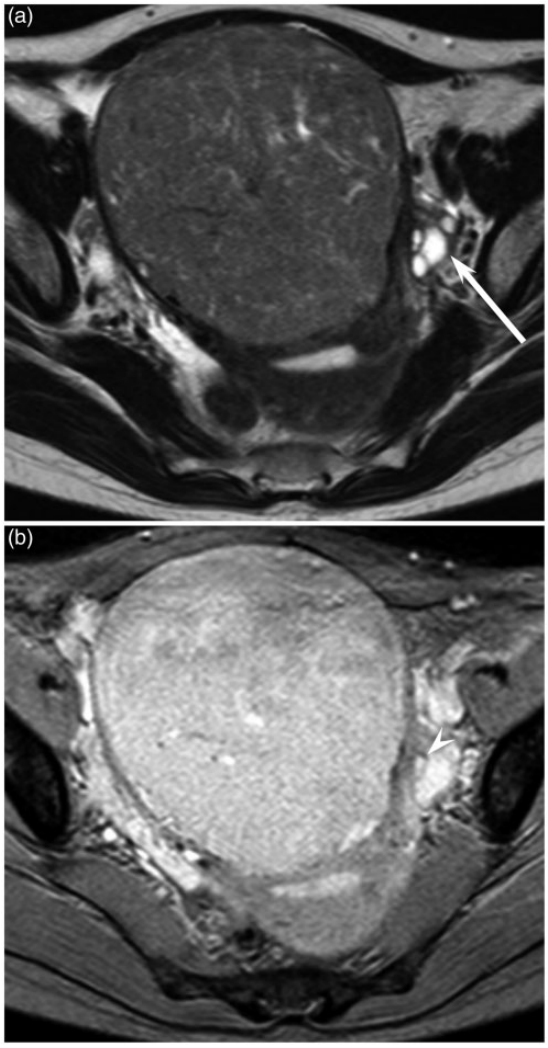


**Fig. 1.** A 41-year-old woman with left untorsed ovary. (a) T2W turbo spin-echo (TR/TE, 4415/100 ms) image shows a left normal ovary (arrow). (b) T2*W gradient-echo (TR/TE, 476/19 ms) image shows ring-shaped hypointensity at the periphery of follicles (arrow head).

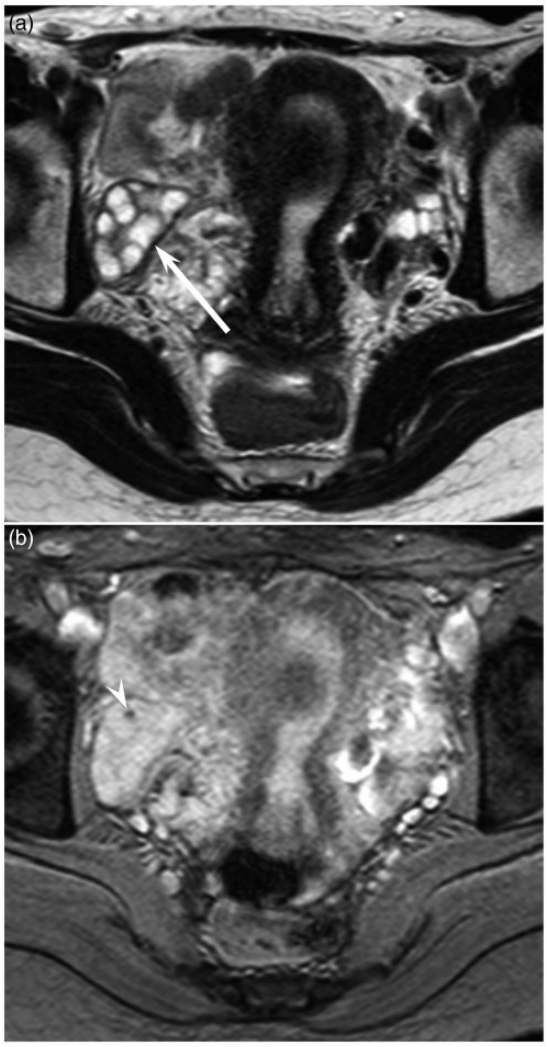


**Fig. 2.** A 36-year-old woman with right untorsed ovary. (a) T2W turbo spin-echo (TR/TE, 4415/100 ms) image shows a right normal ovary (arrow). (b) T2*W gradient-echo (TR/TE, 476/19 ms) image shows punctate hypointensity at the periphery of the follicles (arrow head).

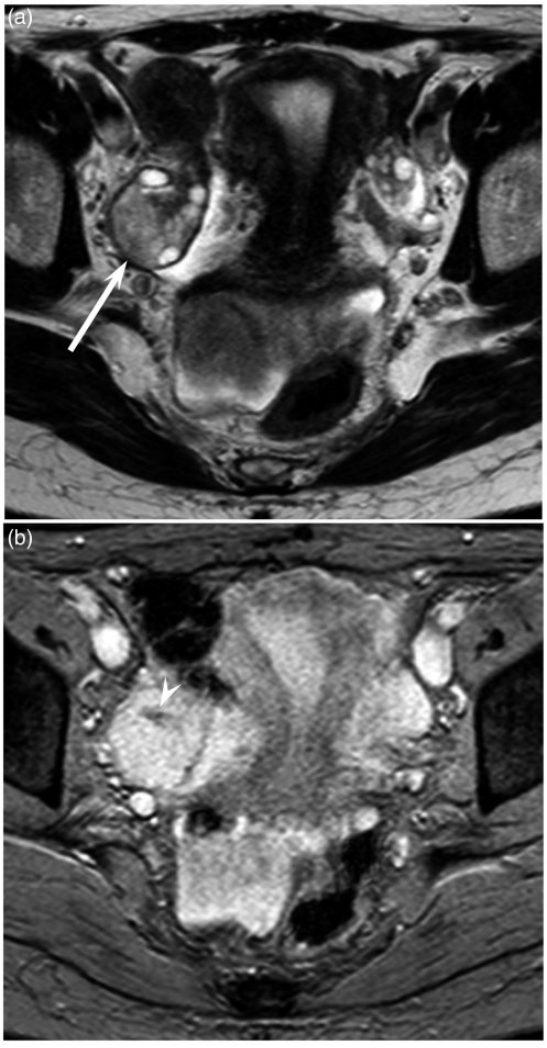


**Fig. 3.** A 40-year-old woman with right untorsed ovary. (a) T2W turbo spin-echo (TR/TE, 4415/100 ms) image shows a right normal ovary (arrow). (b) T2*W gradient-echo (TR/TE, 476/19 ms) image shows patchy hypointensity within ovarian stroma (arrow head).

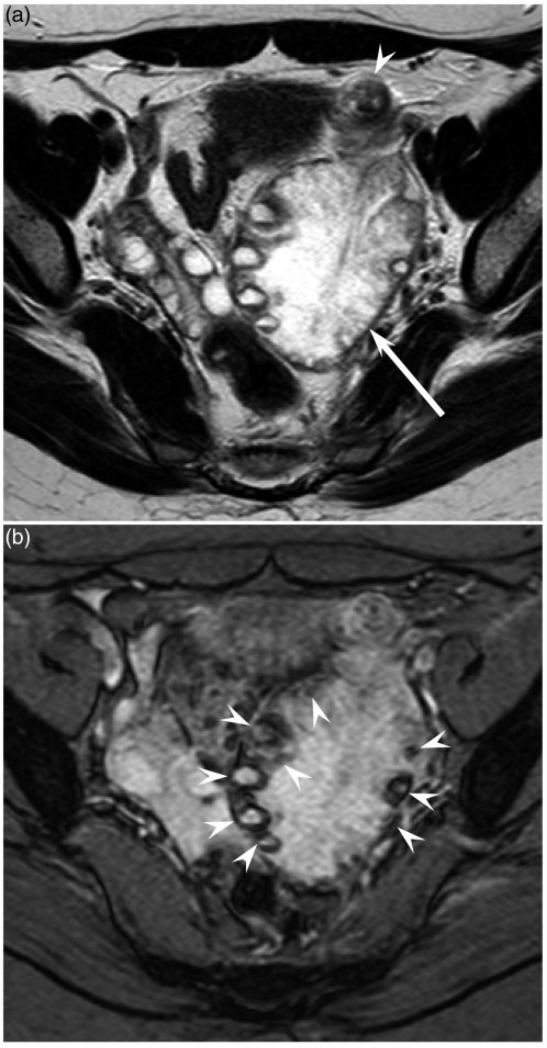


**Fig. 4.** A 36-year-old woman with left torsed ovary without pathology. (a) T2W turbo spin-echo (TR/TE, 4415/100 ms) image shows a left torsed ovary (arrow) with fallopian tube thickening (arrow head). The ovary is enlarged and the follicles are located in the periphery. (b) T2*W gradient-echo (TR/TE, 476/19 ms) image shows diffuse hypointensity at the periphery of the follicles and within ovarian stroma (arrow heads).

to compare quantitative results (patient age, maximum diameter of ovarian stroma, number of follicles, and maximum diameter of follicles). A $P$ value $< 0.05$ was considered to be significant.

## Results

Mean age was significantly lower in patients with adnexal torsion than in those without torsion ($28.8 \pm 11.9$ vs. $38.6 \pm 8.2$ years; $P < 0.01$).

### *Image analysis*

The frequency of hypointensity within the ovarian stroma on T2*W images is shown in Table 1. Hypointensity within the ovarian stroma was present in six of eight (75%) ovaries with torsion and in 26 of 72 (36%) ovaries without torsion; this difference was significant ($P < 0.05$). Hypointensity was observed in all three ovaries with pathologically proven severe hemorrhagic infarction, whereas only three of five (60%) ovaries without severe hemorrhagic infarction demonstrated hypointensity on T2*W images.

The distribution of hypointensity within the ovarian stroma on T2*W images is summarized in Table 2. All 26 ovaries without torsion that had hypointensity on T2*W images were classified as localized: type IA in six, type IB in 17, and type IC in three. Meanwhile, among

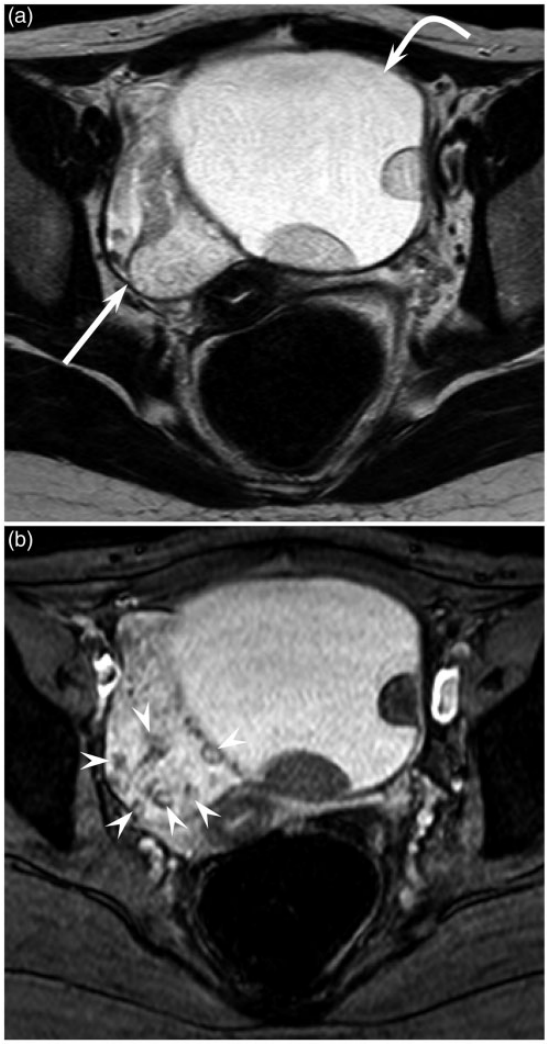


**Fig. 5.** A 15-year-old woman with right torsed normal ovary and left ovarian mature cystic teratoma. (a) T2W turbo spin-echo (TR/TE, 4415/100 ms) image shows a right torsed ovary (arrow) and left ovarian mature cystic teratoma (curved head). (b) T2*W gradient-echo (TR/TE, 476/19 ms) image shows diffuse hypointensity at the periphery of the follicles and within ovarian stroma (arrow heads).

six ovaries with torsion that showed hypointensity, five were classified as diffuse (II) and one was localized (IA). Among the ovaries with hypointensity, the frequency of diffuse distribution was significantly higher in ovaries with torsion than in ovaries without torsion (83% vs. 0%; $P < 0.01$). All ovaries with pathologically proven severe hemorrhagic infarction were classified to have diffuse hypointensity (II).

The maximum diameter of ovarian stroma was significantly higher in ovaries with torsion than in ovaries without torsion ($44.5 \pm 14.5$ mm vs. $26.3 \pm 5.8$ mm; $P < 0.01$). However, there were no significant differences between the two groups in terms of number of follicles ($10.0 \pm 11.8$ vs. $5.2 \pm 4.1$, respectively; $P = 0.29$) and maximum diameter of follicles ($9.0 \pm 5.3$ mm vs. $10.5 \pm 5.2$ mm, respectively; $P = 0.52$). The number of follicles was significantly higher in torsion of normal ovaries than in torsion of ovaries with benign ovarian lesions ($18.8 \pm 11.0$ vs. $1.8 \pm 3.5$; $P < 0.05$).

In eight ovaries with torsion, fallopian tube thickening was observed in seven (88%) and uterine deviation to the side of torsion was observed in four (50%). However, hemoperitoneum was not observed in any of the ovaries.

**Table 1.** Frequency of hypointensity on T2*W images in 80 ovaries.

| | Existence | Non-existence |
|---|---|---|
| Torsed ovary | 6 (75%) | 2 (25%) |
| Untorsed ovary | 26 (36%) | 46 (64%) |

Unless otherwise indicated, data are the number of ovaries, and data in parentheses are the ratio in the groups. Frequency of hypointensity on T2*W images was significantly higher in torsed ovaries than in untorsed ovaries ($P < 0.05$).

**Table 2.** Distribution of hypointensity on T2*W images in 32 ovaries.

| | (I) Localized type | (II) Diffuse type |
|---|---|---|
| Torsed ovary | 1 (17%)<br>(IA); 1<br>(IB); 0<br>(IC); 0 | 5 (83%) |
| Untorsed ovary | 26 (100%)<br>(IIA); 6<br>(IIB); 17<br>(IIC); 3 | 0 (0%) |

Unless otherwise indicated, data are the number of ovaries, and following data in parentheses are the ratio in the groups. The frequency of diffuse distribution was significantly higher in torsed ovaries than in untorsed ovaries ($P < 0.01$).

## Discussion

Most previous studies reported that adnexal torsion was diagnosed based by direct imaging findings, such as twisted or enlarged ovaries, or by indirect imaging findings, such as hemoperitoneum (5–8). In this study, we focused on internal hemorrhage caused by adnexal torsion and performed T2*W MRI of the female pelvis, a gradient-echo imaging that provides superior sensitivity in detecting hemorrhages, compared with conventional spin-echo sequences.

Torsion of the ovarian pedicle produces circulatory stasis, which is initially venous and lymphatic, but eventually becomes arterial and results in the progression of

edema (6). If torsion is complete and arterial blood supply is obstructed, gangrenous and hemorrhagic necrosis occurs. During the progression of torsion, ovarian hemorrhage usually occurs due to venous congestion or hemorrhagic infarction. In our series, T2*W imaging could sensitively demonstrate ovarian hemorrhage by the presence of diffuse hypointensity on T2*W images, which was observed in six of eight ovaries with torsion. Hemosiderin, the final degradation product of hemoglobin in the erythrocytes, has magnetic susceptibility and is shown on T2*W imaging as clear hypointensity. In addition, deoxyhemoglobin or methemoglobin, which appears during the acute or subacute stages of hemorrhage, has magnetic susceptibility. Therefore, T2*W imaging can detect every stage of hemorrhage in the course of adnexal torsion.

In our series, diffuse hypointensity on T2*W images was observed in all ovaries with severe hemorrhagic infarction, but was also seen in ovaries without severe hemorrhagic infarction; the latter finding may be accounted for by venous congestion that was picked up by T2*W images. Therefore, diffuse hypointensity on T2*W images may not always indicate irreversible hemorrhagic infarction in adnexal torsion.

Contrary to our expectations, hypointensity in ovaries without torsion on T2*W images occurred with high frequency. Because ovaries are cyclically hemorrhagic organs, we presumed that hypointensity in ovaries without torsion on T2*W images may be from the hemorrhagic events during the menstrual cycle. Although focal hypointensity was occasionally observed in ovaries without torsion, diffuse hypointensity was not observed. Therefore, diffuse hypointensity on T2*W images may be specific for adnexal torsion.

In ovaries without torsion with hypointensity on T2*W images, the most frequent distribution of hypointensity on T2*W images was type IB, followed by type IA. Because the periphery of the follicles is usually the location of ring-like enhancement on contrast-enhanced CT or MR images, this area is believed to receive abundant blood supply; however, it is also sensitive to ischemia. Therefore, we assumed that hypointensity in ovaries without torsion on T2*W images had a tendency to be located at the periphery of the follicles.

Our study had several limitations. First, our study population, particularly in patients with adnexal torsion, was small because of the rarity of this disease. Second, pathological confirmation of hemorrhagic infarction was available in only three ovaries because the other diseased ovaries could be salvaged in a viable state. Conservative operations, like laparoscopic repair, have been recently performed to preserve ovarian function (17–19). Also, future research should include comparison of this sign to the other, and to check the inter-observer reproducibility of this finding. Third, other hemorrhagic lesions, such as hemorrhagic cysts and endometriomas, were not analyzed. They may present with similar clinical symptoms. How they show on T2*W images was not clear.

In conclusion, the frequency of hypointensity on T2*W images was significantly higher in ovaries with torsion than in ovaries without torsion. Diffuse hypointensity was significantly more frequent in ovaries with torsion than in ovaries without torsion and was observed in all cases with pathologically-proven severe hemorrhagic infarction, but not in those without torsion. The presence and distribution of hypointensity on T2*W imaging may play a supplementary role in the detection of adnexal torsion. T2*W imaging should be included in patients with suspicion of adnexal torsion.

## Declaration of conflicting interests

The author(s) declared no potential conflicts of interest with respect to the research, authorship, and/or publication of this article.

## Funding

The author(s) received no financial support for the research, authorship, and/or publication of this article..

## References

1. Hiller N, Appelbaum L, Simanovsky N, et al. CT features of adnexal torsion. Am J Roentgenol 2007;189:124–129.
2. Chang HC, Bhatt S, Dogra VS. Pearls and pitfalls in diagnosis of ovarian torsion. Radiographics 2008;28: 1355–1368.
3. Rha SE, Byun JY, Jung SE, et al. CT and MR imaging features of adnexal torsion. Radiographics 2002;22: 283–294.
4. Lourenco AP, Swenson D, Tubbs RJ, et al. Ovarian and tubal torsion: imaging findings on US, CT, and MRI. Emerg Radiol 2014;21:179–187.
5. Kimura I, Togashi K, Kawakami S, et al. Ovarian torsion: CT and MR imaging appearances. Radiology 1994; 190:337–341.
6. Jain KA. Magnetic resonance imaging findings in ovarian torsion. Magn Reson Imaging 1995;13:111–113.
7. Bader T, Ranner G, Haberlik A. Torsion of a normal adnexa in a premenarcheal girl: MRI findings. Eur Radiol 1996;6:704–706.
8. Cheng KL, Tsao TF. Ovarian torsion: appearance on MRI. Pediatr Radiol 2010;40:S104.
9. Beranger-Gibert S, Sakly H, Ballester M, et al. Diagnostic value of MR imaging in the diagnosis of adnexal torsion. Radiology 2015;279:461–470.
10. Lin DD, Filippi CG, Steever AB, et al. Detection of intracranial hemorrhage: comparison between gradient-echo images and b(0) images obtained from diffusion-weighted echo-planar sequences. Am J Neuroradiol 2001;22: 1275–1281.

11. Tsushima Y, Aoki J, Endo K. Brain microhemorrhages detected on T2*-weighted gradient-echo MR images. Am J Neuroradiol 2003;24:88–96.
12. Chan S, Kartha K, Yoon SS, et al. Multifocal hypointense cerebral lesions on gradient-echo MR are associated with chronic hypertension. Am J Neuroradiol 1996;17: 1821–1827.
13. Gomori JM, Grossman RI, Goldberg HI, et al. Intracranial hematomas: imaging by high-field MR. Radiology 1985;157:87–93.
14. Bradley WG Jr. MR appearance of hemorrhage in the brain. Radiology 1993;189:15–26.
15. Hermier M, Nighoghossian N. Contribution of susceptibility-weighted imaging to acute stroke assessment. Stroke 2004;35:1989–1994.
16. Takeuchi M, Matsuzaki K, Harada M. Susceptibility-weighted imaging of ovarian torsion: a case report. Magn Reson Med Sci 2015;14:355–358.
17. Rousseau V, Massicot R, Darwish AA, et al. Emergency management and conservative surgery of ovarian torsion in children: a report of 40 cases. J Pediatr Adolesc Gynecol 2008;21:201–206.
18. Galinier P, Carfagna L, Delsol M, et al. Ovarian torsion. Management and ovarian prognosis: a report of 45 cases. J Pediatr Surg 2009;44:1759–1765.
19. Geimanaite L, Trainavicius K. Ovarian torsion in children: management and outcomes. J Pediatr Surg 2013;48: 1946–1953.